DOI: 10.1002/chem.201000362

Cationic Iridium(III) Complex Containing both Triarylboron and Carbazole Moieties as a Ratiometric Fluoride Probe That Utilizes a Switchable Triplet–Singlet Emission

Wen-Juan Xu,[a] Shu-Juan Liu,[a] Xin-Yan Zhao,[a] Shi Sun,[a] Shan Cheng,[a] Ting-Chun Ma,[a] Hui-Bin Sun,[a] Qiang Zhao,*[a, b] and Wei Huang*[a]

Abstract: A novel cationic Ir^{III} complex $[Ir(Bpq)_2(CzbpyCz)]PF_6$ (Bpq = 2-[4-(dimesitylboryl)phenyl]quinoline, CzbpyCz = 5,5′-bis(9-hexyl-9*H*-carbazol-3-yl)-2,2′-bipyridine) containing both triarylboron and carbazole moieties was synthesized. The excited-state properties of $[Ir(Bpq)_2(CzbpyCz)]PF_6$ were investigated through UV/Vis absorption and photoluminescence spectroscopy and molecular-orbital calculations. This complex displayed highly efficient orange-red phosphorescent emission with an emission peak of 583 nm and quantum efficiency of $\Phi = 0.30$ in dichloromethane at room temperature. The binding of fluoride ions to $[Ir(Bpq)_2(CzbpyCz)]PF_6$ can quench the phosphorescent emission from the Ir^{III} complex and enhance the fluorescent emission from the N^N ligand, which corresponds to a visual change in the emission from orange-red to blue. Thus, both colorimetric and ratiometric fluoride sensing can be realized. Interestingly, an unusual intense absorption band in the visible region was observed. And the detection of F^- ions can also be carried out with visible light as the excitation wavelength. More importantly, the linear response of the probe absorbance change at $\lambda = 351$ nm versus the concentration of F^- ions allows efficient and accurate quantification of F^- ions in the range 0–50 μM.

Keywords: boron · iridium · luminescence · phosphorescence · sensors

Introduction

Among the anions, the fluoride ion is attracting particular interest because it can be considered as both a dangerous pollutant and useful additive in industrial processes and the human diet. In addition, fluoride ions play an essential role in a broad range of biological, medical, and chemical processes and in applications such as dental care, treatment of osteoporosis, fluorination of water supplies, and even chemical and nuclear warfare agents.[1] Consequently, the recognition and detection of F^- ions are of growing interest and there is a need to develop new selective and sensitive methods for the detection of F^- ions in various environments; therefore, many sensing techniques have been developed for the purpose of detecting F^- ions. Among these sensing techniques, fluorescent detection is considered to be one of the most effective tools owing to its high sensitivity, easy visualization, and short response time for detection. Up until now, a large number of organic luminophores have been designed as probes for this important analyte,[2] and most fluorescent probes are based on variation in the luminescent intensity. Although these intensity-based probes are of practical utility, external influences that lead to variations in probe concentration and environment can complicate measurements in practical application. The potential interference can be minimized by ratiometric detection, which relies on probes that have two distinct measurable signals in the presence or absence of the analyte.[2a]

---

[a] W.-J. Xu, Dr. S.-J. Liu, X.-Y. Zhao, S. Sun, S. Cheng, T.-C. Ma,
H.-B. Sun, Dr. Q. Zhao, Prof. W. Huang
Jiangsu Key Laboratory for Organic Electronics & Information
Displays and Institute of Advanced Materials (IAM)
Nanjing University of Posts & Telecommunications (NUPT)
9 Wenyuan Road, Nanjing 210046 (China)
Fax: (+86) 25-85866396
E-mail: wei-huang@njupt.edu.cn
iamqzhao@njupt.edu.cn

[b] Dr. Q. Zhao
State Key Laboratory of Coordination Chemistry
Nanjing University
Nanjing, 210093 (China)

Supporting information for this article is available on the WWW under http://dx.doi.org/10.1002/chem.201000362.

The design principles of most fluorescent F^- probes are based on the formation of a hydrogen bond between the active N–H group of organic luminophores and F^- ions.[3] Recently, specific Lewis acid/base interactions, such as the strong affinity of a boron atom toward F^- ions, have been adopted as an efficient approach for fluoride detection.[2a–d] In particular, three-coordinated boron compounds with a dimesitylboryl ($BMes_2$) group are highly selective colorimetric chemosensors for F^- ions.[2a–d, 4]

In addition to the widely used organic luminophores, most recently, phosphorescent heavy-metal complexes have been applied successfully in the field of chemosensors[5] as a result of their advantageous photophysical properties, such as the sensitivity of emission properties to changes in the local environment, evident Stokes shifts for easy separation of excitation and emission, significant single-photon excitation in the visible range, and relatively long lifetimes relative to those of purely organic luminophores. The relatively long lifetime of these heavy-metal complexes (from the order of microseconds to milliseconds) can also endow them with a capacity for excellent temporal resolution, so their luminescence can be easily separated from fluorescent backgrounds and consequently the signal–noise ratio can be increased. In addition, relative to purely organic luminophores, the excited-state properties of phosphorescent heavy-metal complexes are more complicated and depend on the metal center, chemical structures, and the triplet-state energy levels of the ligands. If the ligand of a heavy-metal complex contains a specific coordinating element for an analyte, the presence of this analyte can lead to dramatic variation in the photophysical and electrochemical properties of the complex, thus realizing detection. According to this principle, we have successfully realized excellent phosphorescent probes for Hg^{2+} ions, anions, and homocysteine.[6] In addition, the introduction of $BMes_2$ groups into the ligand of phosphorescent heavy-metal complexes can also realize novel phosphorescent F^- probes through the specific interaction of the boron atom with F^- ions, which can induce variations in the excited-state properties of heavy-metal complexes.[6c, 7]

As a class of novel phosphorescent material, there have been several investigations into phosphorescent Cu^I, Pt^{II}, Re^I, Ru^{II}, and Ir^{III} complexes containing $BMes_2$ groups by us and others over the past three years.[6c, 7] Most of these reports are based on the principle of incorporating $BMes_2$ groups into the conjugated structure of the ligand and that binding with F^- ions induces variation in the phosphorescent signal. Most recently, Wang and co-workers observed an interesting ambient-temperature singlet–triplet dual emission for nonconjugated donor–acceptor triarylboron–Pt^{II} complexes (see Figure 1a).[7g] Furthermore, binding of F^- ions can increase both the singlet and triplet emissions, and the enhanced degree of triplet emission is higher than that of the singlet emission. Therefore, how to design ratiometric probes with a switchable triplet–singlet emission is very interesting. However, up until now, there have been no reports on the realization of such ratiometric probes that utilize a triplet–singlet emission switch for phosphorescent heavy-metal complexes containing $BMes_2$ groups in the conjugated structure of the ligand (Figure 1b).

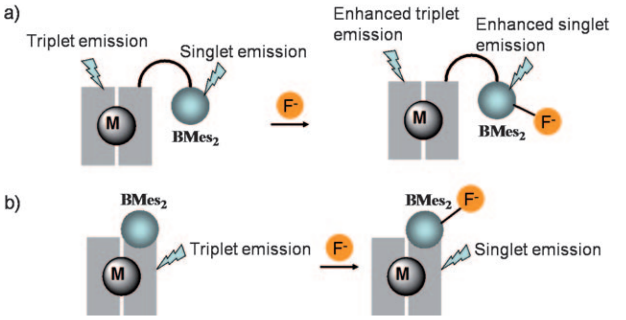

Figure 1. Phosphorescent F^- probes based on heavy-metal complexes containing the $BMes_2$ group with nonconjugated (a) and conjugated (b) structures utilizing triplet–singlet dual emissions.

Herein, we have designed and synthesized the novel cationic Ir^{III} complex $[Ir(Bpq)_2(CzbpyCz)]PF_6$ (Bpq = 2-[4-(dimesitylboryl)phenyl]quinoline, CzbpyCz = 5,5′-bis(9-hexyl-9*H*-carbazol-3-yl)-2,2′-bipyridine; Scheme 1) with dimesitylboryl groups on the cyclometalated C^N ligands (Bpq). The 2,2-bipyridine-based oligomer CzbpyCz with carbazole units was selected as an N^N ligand that can act as energy donor. Different from the work of Wang and co-workers, the energy donor and acceptor were incorporated into the complex through a conjugated binding approach. The ratiometric and colorimetric detection of F^- ions was realized by switchable fluorescence and phosphorescence from the N^N ligand and complex, respectively. Interestingly, an unusual intense absorption band in the visible region was observed. Therefore, the detection of F^- ions can also be carried out with visible light as the excitation wavelength.

Results and Discussion

Synthesis and characterization of $[Ir(Bpq)_2(CzbpyCz)]PF_6$: Scheme 1 shows the synthetic route to the target Ir^{III} complex $[Ir(Bpq)_2(CzbpyCz)]PF_6$. The N^N ligand CzbpyCz was synthesized from 9-hexyl-9*H*-carbazol-3-ylboronic acid and 5,5′-dibromo-2,2′-bipyridine by using the Suzuki–Miyaura cross-coupling reaction.[8] The synthesis of the cyclometalated C^N ligand Bpq comprises two steps: First, precursor 2-(4-bromophenyl)quinoline (Brpq) was easily obtained in good yield by a Friedländer condensation reaction of 2-aminobenzadehyde with 4-bromoacetophenone according to a previously reported procedure.[9] Second, ligand Bpq was synthesized in 60 % yield by lithiating Brpq, followed by the addition of dimesitylboron fluoride (Mes_2BF) at −78 °C.[10] The dinuclear cyclometalated Ir^{III} chloro-bridged precursor $[\{Ir(Bpq)_2Cl\}_2]$ with Bpq as a cyclometalated ligand was synthesized by using the same method as Nonoyama.[11] The cationic Ir^{III} complex was routinely synthesized in high yields of 70 % by treating the cyclometalated Ir^{III} chloro-bridged precursor with the CzbpyCz ligand. The structure of

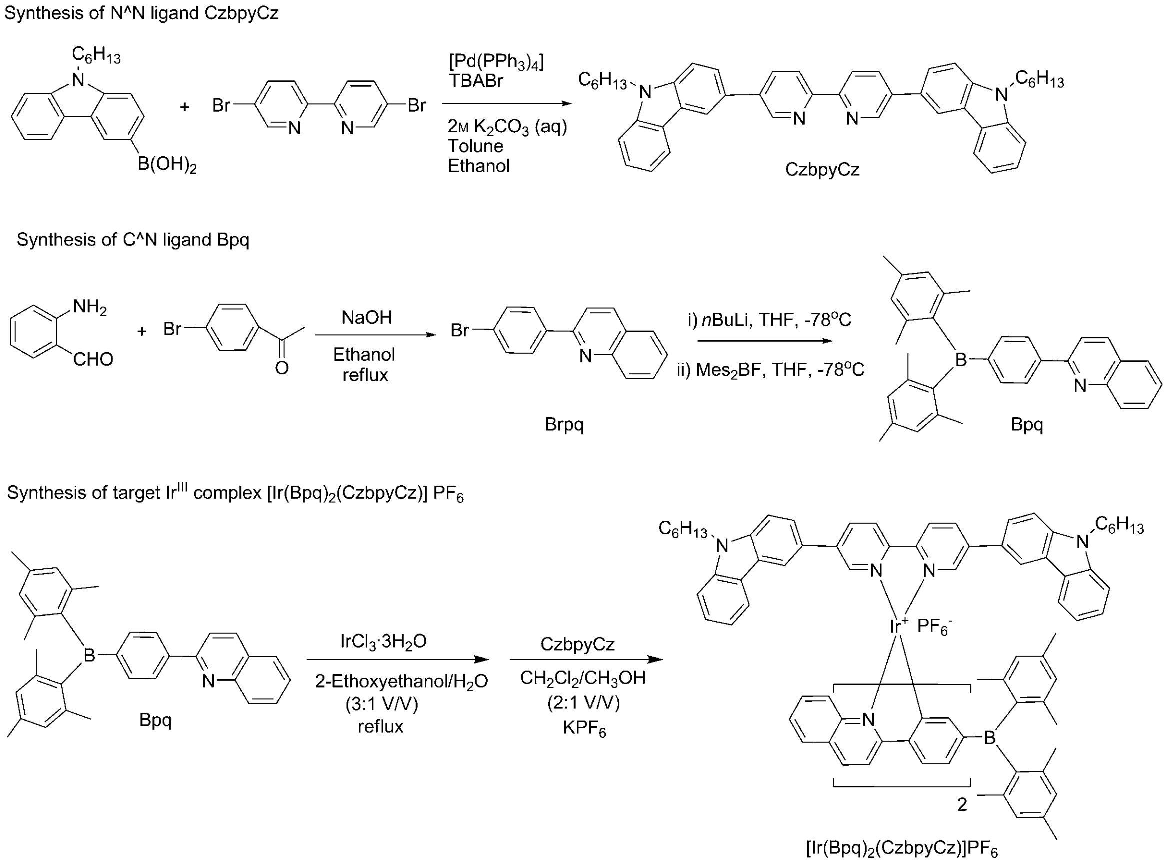

Scheme 1. The synthetic route to [Ir(Bpq)$_2$(CzbpyCz)]PF_6. TBABr = tetrabutylammonium bromide.

the target complex was characterized by ^{1}H and ^{13}C NMR spectroscopic and MALDI-TOF mass spectrometry.

Photophysical properties of the N^N ligand CzbpyCz: The UV/Vis absorption and photoluminescent (PL) spectra of the CzbpyCz ligand are shown in Figure 2 and the data are summarized in Table 1, which are also compared with bipyridine. Relative to bipyridine, CzbpyCz showed redshifted and intense absorption bands centered at $\lambda = 245$, 300, and 353 nm with molar extinction coefficients of $\varepsilon > 10^4\,\mathrm{mol^{-1}\,dm^3\,cm^{-1}}$. The absorption bands centered at $\lambda = 245$ and 300 nm of CzbpyCz can be assigned to π–π* transitions from the bipyridine and carbazole units. To clarify the origin of the intense absorption band at $\lambda = 353$ nm, molecular-orbital calculations for CzbpyCz were performed by using time-dependent density functional theory (TDDFT) calculations (see Figure 3). According to the calculation results, the HOMO is mainly localized at the carbazole moieties with some contribution from the bipyridine unit, and the LUMO is localized at the bipyridine moiety. The absorption of CzbpyCz at $\lambda = 353$ nm is mainly attributed to a

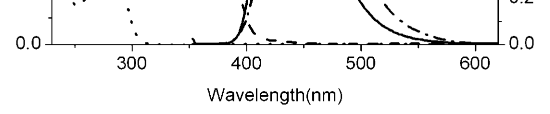

Figure 2. UV/Vis absorption spectra of bipyridine and CzbpyCz moieties, and the PL spectra of CzbpyCz under different conditions at room temperature.

Table 1. Photophysical data for CzbpyCz and [Ir(Bpq)$_2$(CzbpyCz)]PF_6 at 298 K.

Compound	λ_{abs} [nm] (log ε)	λ_{em} [nm] (CH_2Cl_2)	λ_{em} [nm] (CH_3CN)	Φ[a]	τ [μs]
Bpy	235(4.11), 281(4.21)				
CzbpyCz	245(4.52), 300(4.46), 353(4.62)	436	450	0.83	
[Ir(Bpq)$_2$(CzbpyCz)]PF_6	268(4.89), 291(4.93), 351(4.74), 430(4.62)	583	584	0.30	1.96

[a] The quantum efficiency for CzbpyCz was obtained under air with 9,10-diphenylanthracene as an external standard; the quantum efficiency for [Ir(Bpq)$_2$(CzbpyCz)]PF_6 was measured under N_2 with [Ir(ppy)$_3$] as an external standard (Φ = 0.40).[12]

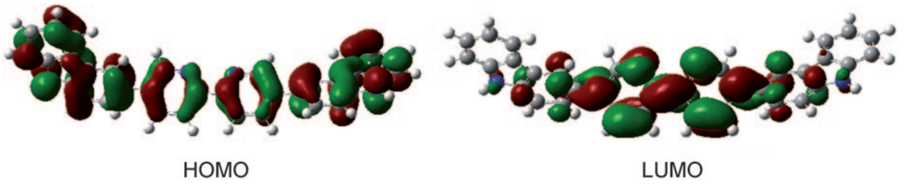

Figure 3. HOMO and LUMO orbitals of CzbpyCz.

HOMO→LUMO excitation. Therefore, the lowest electronic transition of CzbpyCz can be mainly assigned to a charge-transfer (CT) state from the carbazole to bipyridine units with a π–π* transition of the bipyridine moiety.

It can be seen that CzbpyCz displayed an intense-blue emission in CH_2Cl_2 with a maximal emission wavelength at $\lambda = 436$ nm and a quantum efficiency of $\Phi = 0.83$ (Figure 2). In addition, the emission spectrum of CzbpyCz has a dependence on the solvent polarity as the λ_{max} value shifts to $\lambda = 450$ nm in CH_3CN, thus indicating the CT character of the excited state, which is in accordance with the TDDFT calculation results.

Photophysical properties of $[Ir(Bpq)_2(CzbpyCz)]PF_6$: The UV/Vis absorption and PL spectra of $[Ir(Bpq)_2(CzbpyCz)]PF_6$ are shown in Figure 4 and the data are summarized in Table 1. The complex displayed intense absorption bands at $\lambda = 250$–400 nm, related to the singlet ligand-centered π–π* transitions from the Bpq and CzbpyCz ligands. Interestingly, the complex showed an unusual intense absorption band at $\lambda = 430$ nm with $\varepsilon > 10^4\,mol^{-1}\,dm^3\,cm^{-1}$. As confirmed by TDDFT calculations (see Figure 5 and Table 2), this intense absorption at $\lambda = 430$ nm mainly originates from the S_4 state, namely, HOMO→LUMO and HOMO−1→LUMO transitions, thus corresponding to CT character from the HOMO and HOMO−1 that reside on the carbazole fragment to the LUMO localized on the bipydrine fragment, which is similar to the CT transition of the free CzbpyCz ligand in $\lambda = 353$ nm, except that the λ_{max} value of this band in the complex is red-shifted. In addition, the weak absorption bands of the complex in the region $\lambda = 450$–550 nm can be assigned to a mixture of ligand-to-ligand charge-transfer (LLCT), metal-to-ligand charge-transfer (MLCT), and ligand-centred (LC) transitions.

Complex $[Ir(Bpq)_2(CzbpyCz)]PF_6$ showed an intense emission band at about $\lambda = 583$ nm with an orange-red emission at room temperature in CH_2Cl_2, which had little dependence on the solvent polarity and temperature (Figure 4). According to previous studies on cationic Ir^{III} complexes containing diimine ligands, their excited states are very complicated and the emission often comes from mixed excited states containing ^{3}LC, ^{3}MLCT, and ^{3}LLCT transitions.[13] The emissions from ligand-centred ^{3}LC(π–π*) states often

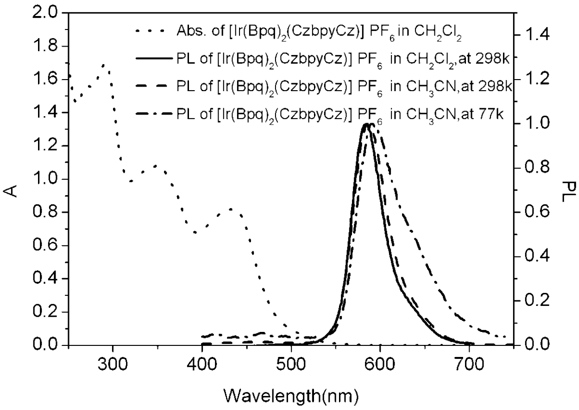

Figure 4. UV/Vis absorption spectra and the normalized emission spectra of $[Ir(Bpq)_2(CzbpyCz)]PF_6$ under different conditions.

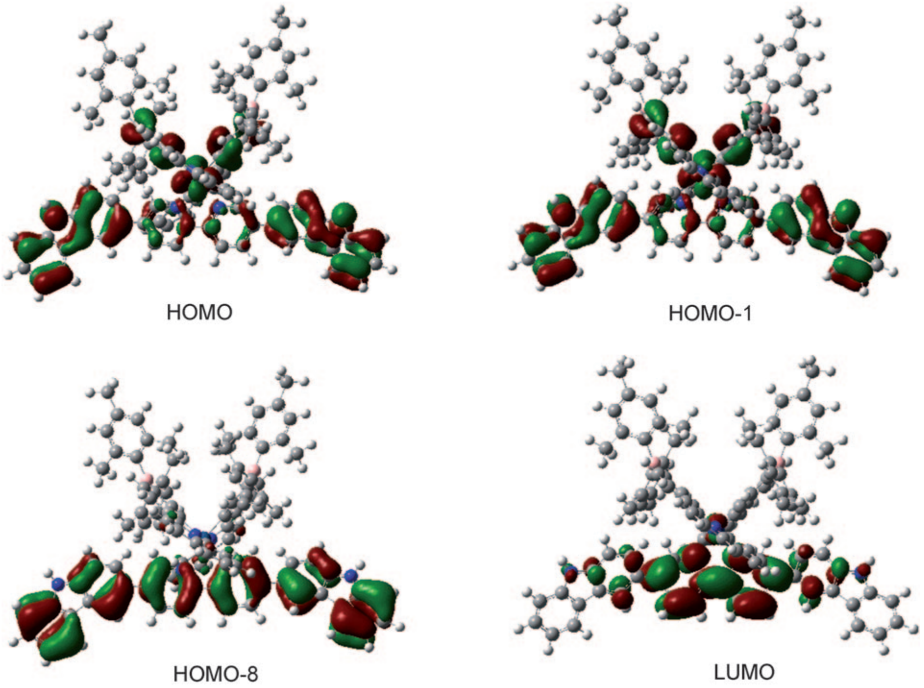

Figure 5. HOMO, HOMO−1, HOMO−8, and LUMO orbitals of $[Ir(Bpq)_2(CzbpyCz)]PF_6$.

Table 2. Calculated energy levels of the lowest singlet and triplet states for $[Ir(Bpq)_2(CzbpyCz)]PF_6$.

State	Excitation	E_{calcd}[a] [eV]	λ_{calcd}[a] [nm]	f[b]
S1	HOMO−1→LUMO (46 %) HOMO→LUMO (52 %)	2.33	531	0.0123
S2	HOMO−1→LUMO+1 (46 %) HOMO→LUMO+1 (51 %)	2.49	497	0.0022
S3	HOMO−1→LUMO+2 (46 %) HOMO→LUMO+2 (50 %)	2.50	495	0.0420
S4	HOMO−1→LUMO (52 %) HOMO→LUMO (45 %)	2.62	473	0.68
T1	HOMO−8→LUMO (20 %) HOMO→LUMO (64 %)	2.19	567	0

[a] E_{calcd}: calculated energy. [b] f: calculated oscillator strength.

display vibronic progressions and small dependence on solvent polarity and temperature, whereas those emissions from CT states are often broad, featureless, and sensitive to solvent polarity and temperature.[13,14] No vibronic progressions were observed, thus indicating that the excited state of the complex has some CT character. In addition, the PL spectra of $[Ir(Bpq)_2(CzbpyCz)]PF_6$ are insensitive to solvent polarity and temperature, thus indicating that the ^{3}LC transition dominates in the excited states. The phosphorescence quantum yield in degassed CH_2Cl_2 is $\Phi = 0.30$, and the emission lifetime at $\lambda = 583$ nm is $\tau = 1.96$ µs, thus indicating the phosphorescent nature of the emission.

Molecular orbital calculations for $[Ir(Bpq)_2(CzbpyCz)]PF_6$ were performed by using TDDFT calculations (Figure 5 and Table 2). The lowest triplet state (T_1) of $[Ir(Bpq)_2(CzbpyCz)]PF_6$ originates from HOMO→LUMO and HOMO−8→LUMO transitions. The HOMO distribution primarily resides on the carbazole fragments with some localized on the phenyl rings of the cyclometalated ligands and the Ir^{III} center, and the HOMO−8 distribution primarily resides on the CzbpyCz ligand. The LUMO distribution is dominated by the bipyridine fragment. Hence, the lowest triplet state apparently possesses more ligand-centred (N^N ligand) character (^{3}LC) and mixes with some $\pi_{phenyl} \rightarrow \pi^*_{N\hat{}N}$ (^{3}LLCT) and $d\pi_{(Ir\ center)} \rightarrow \pi^*_{N\hat{}N}$ (^{3}MLCT) transitions, which is in accordance with the emission character.

Optical responses of $[Ir(Bpq)_2(CzbpyCz)]PF_6$ to F^- ions: The response of $[Ir(Bpq)_2(CzbpyCz)]PF_6$ to F^- ions was investigated through UV/Vis absorption and emission spectroscopic analysis. Figure 6 shows the variation in the absorption spectra of $[Ir(Bpq)_2(CzbpyCz)]PF_6$ upon the addition of F^- ions. The absorptions at $\lambda = 291$ and 351 nm decreased gradually, whereas the absorption at $\lambda = 414$ nm increased gradually, which corresponds to an isobestic point at $\lambda = 379$ nm. Additionally, the absorbance at $\lambda = 430$–550 nm decreased gradually, thus corresponding to another isobestic point at $\lambda = 430$ nm.

The variation in the PL spectra with $\lambda = 379$ nm as the excitation wavelength is shown in Figure 7a. Upon the addition of F^- ions to a solution of $[Ir(Bpq)_2(CzbpyCz)]PF_6$ in CH_3CN, the phosphorescent emission intensity at $\lambda = 584$ nm decreased gradually and was blueshifted to $\lambda = 572$ nm, whereas the emission intensity at $\lambda = 458$ nm, which is tentatively attributed to the emission of the CzbpyCz ligand, in-

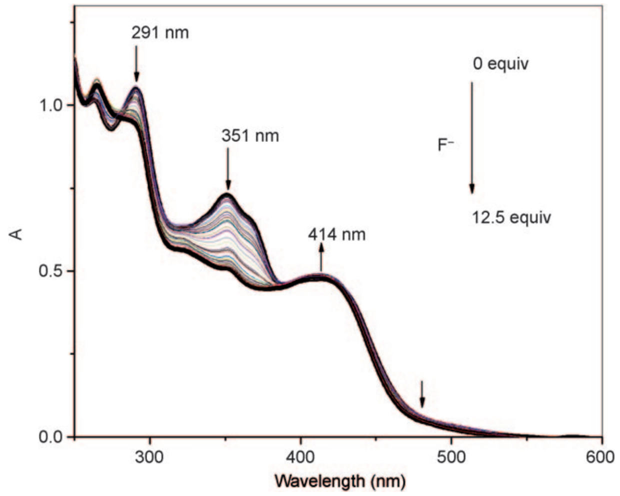

Figure 6. Change in the UV/Vis absorption spectra of $[Ir(Bpq)_2(CzbpyCz)]PF_6$ (20 µM) in CH_3CN with various amounts of F^- ions.

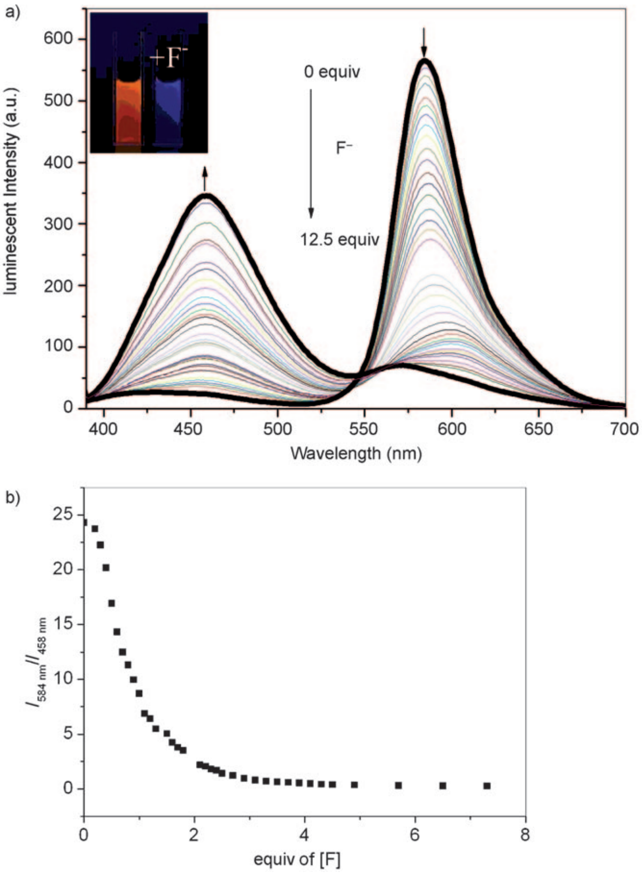

Figure 7. a) Change in the emission spectra of $[Ir(Bpq)_2(CzbpyCz)]PF_6$ (20 µM) in CH_3CN with various amounts of F^- ions excited at $\lambda = 379$ nm. Inset: color of the emission observed of $[Ir(Bpq)_2(CzbpyCz)]PF_6$ in CH_3CN (20 µM) in the absence (left) and presence (right) of F^- ions. b) Fluorescent titration profile of I_{584}/I_{458} versus the equivalents of F^- ions added.

creased gradually with a clear isoemission point at $\lambda=540$ nm, thus realizing ratiometric F^- sensing. The ratios of emission intensities at $\lambda=584$ and 458 nm (I_{584}/I_{458}) exhibit a dramatic change from 24.0:1 to 0.4:1. Such a large change of emission intensity ratios at two wavelengths is desirable for ratiometric fluorescent probes, as the sensitivity and the dynamic range of ratiometric probes are controlled by the emission ratio. Furthermore, the difference in the two emission wavelength is very large ($\lambda=126$ nm). This difference not only contributes to the accurate measurement of two emission intensities, but also results in a huge ratiometric value. More interestingly, an obvious change of emission color from orange/red to blue was observed (Figure 7a, inset), thus enabling colorimetric F^- sensing. The short emission lifetime ($\tau=5.71$ and 1.18 ns) of the new blue emission at $\lambda=458$ nm indicates the fluorescent nature of the complex. Furthermore, the emission wavelength and band shape of the blue emission are similar to those of the N^N ligand CzbpyCz, thus indicating that the blue emission at $\lambda=458$ nm originates from the singlet emission of CzbpyCz. That is to say, binding of F^- ions to [Ir(Bpq)$_2$(CzbpyCz)]PF$_6$ quenched the triplet emission from the Ir^{III} complex and switched on the singlet emission from the N^N ligand.

After the addition of approximately two equivalents of F^- ions, the emission intensity ratio of I_{584}/I_{458} reaches saturation point (see the emission titration curves in Figure 7b). Considering that there are two boron centers in one molecule of the complex, it is possible for [Ir(Bpq)$_2$(CzbpyCz)]PF$_6$ to form a 1:2 complex with two equivalents of F^- ions because the two dimesitylboryl groups are electronically separated in the ground state and spatially distant from each other. Using the UV/Vis titration data, the binding constants (K_1 and K_2) of the Ir^{III} complex were determined to be 6.60×10^5 and $2.04\times10^3\,\text{M}^{-1}$, respectively, which are similar to the values reported previously for boryl-based fluorescent and phosphorescent receptors.[2d,6c]

One of the challenges in the design of luminescent chemosensors, particularly those aimed at bioanalysis and practical application, is to shift the excitation wavelength from the UV region to the visible range because a lot of background fluorescence can not be excited by visible light and visible excitation requires cheaper optical cells and optics. In view of the strong absorption of [Ir(Bpq)$_2$(CzbpyCz)]PF$_6$ within the visible region, the variation in the PL spectra of [Ir(Bpq)$_2$(CzbpyCz)]PF$_6$ responsive to F^- ions excited at $\lambda=430$ nm was investigated. The orange-red emission at $\lambda=584$ nm of [Ir(Bpq)$_2$(CzbpyCz)]PF$_6$ decreased gradually and was blueshifted to $\lambda=572$ nm on the addition of F^- ions, whereas the blue emission at $\lambda=458$ nm was not observed, thus indicating that the detection excited by visible light was also realized (Figure 8).

Quantification of F^- ions: To quantify the concentration of F^- ions in solution, the change in the absorption spectra is correlated to the analyte concentration by using $f=(A_0-A)/A_0$, where A and A_0 are the absorbances at $\lambda=351$ nm in the presence and absence of F^- ions, respectively (Figure 6).

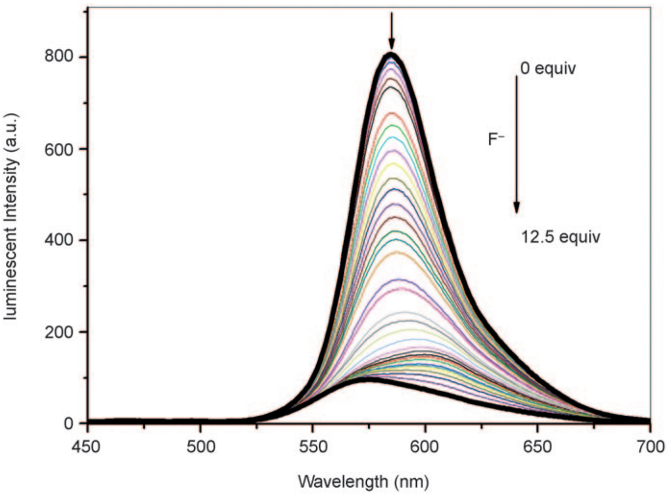

Figure 8. Change in the emission spectra of [Ir(Bpq)$_2$(CzbpyCz)]PF$_6$ (20 μM) in CH$_3$CN with various amounts of F^- ions excited at $\lambda=430$ nm.

The calibration factor f is defined to minimize the influence of the absorption background in the absence of F^- ions. Figure 9 shows f as a function of the concentration of F^- ions in CH$_3$CN. Complex [Ir(Bpq)$_2$(CzbpyCz)]PF$_6$ gives a linear response for F^- ions at 0–50 μM and the correlation coefficient is 0.99, which is suitable for monitoring F^- ions and quantification at 0–50 μM (Figure 9).

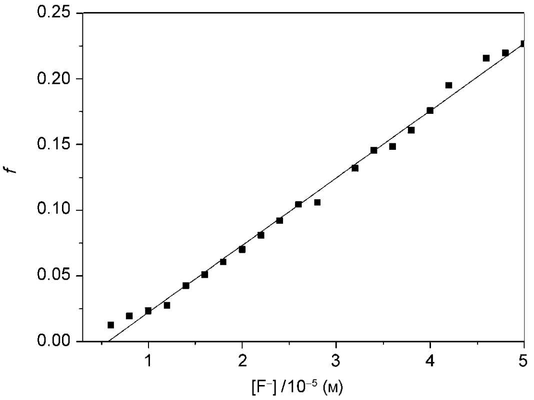

Figure 9. A plot of f as a function of the concentration of F^- ions for [Ir(Bpq)$_2$(CzbpyCz)]PF$_6$ (20 μM) in CH$_3$CN at room temperature.

Sensing mechanism of [Ir(Bpq)$_2$(CzbpyCz)]PF$_6$: Molecular orbital calculations for the adduct [Ir(Bpq)$_2$(CzbpyCz)]PF$_6$·2F^- were performed by using TDDFT calculations to better understand the sensing mechanism of [Ir(Bpq)$_2$(CzbpyCz)]PF$_6$ (see Figure 10 and Scheme 2). For the adduct, the lowest triplet state originates from HOMO−2→LUMO (50%) and HOMO−4→LUMO (36%) transitions. The HOMO−2 and HOMO−4 distributions primarily reside on the BMes$_2$–F^- fragments, and the LUMO distribution resides on the bipyridine fragment. Therefore, the T$_1$ of

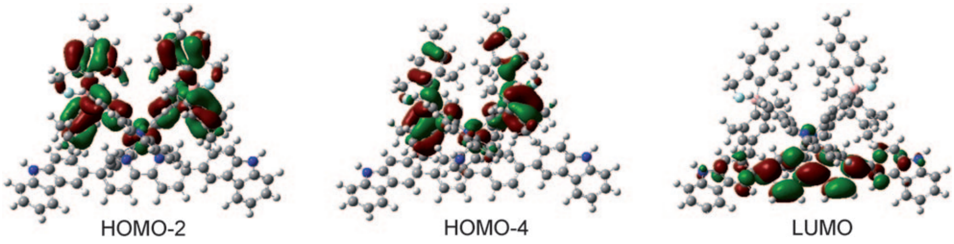

Figure 10. HOMO−2, HOMO−4, and LUMO orbitals of [Ir(Bpq)$_2$(CzbpyCz)]PF$_6$·2F$^-$.

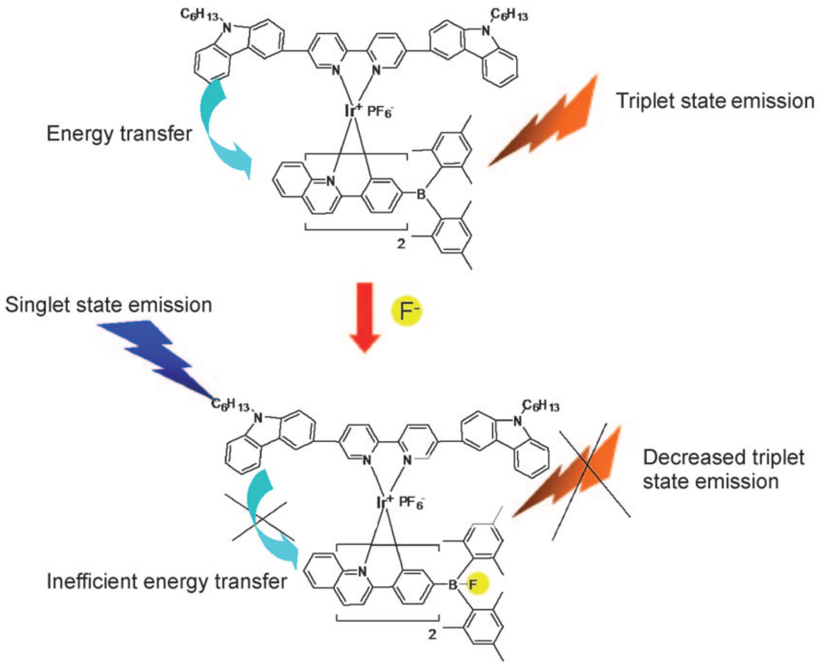

Scheme 2. The sensing mechanism of [Ir(Bpq)$_2$(CzbpyCz)]PF$_6$ to F$^-$ ions.

[Ir(Bpq)$_2$(CzbpyCz)]PF$_6$·2F$^-$ can be assigned to the ^{3}LLCT transition from the BMes$_2$ group to the N^N ligand. We tentatively think that this transition is responsible for the emission at $\lambda = 572$ nm of [Ir(Bpq)$_2$(CzbpyCz)]PF$_6$ after binding with F$^-$ ions.

The PL spectra of the CzbpyCz ligand, [Ir(Bpq)$_2$(CzbpyCz)]PF$_6$, and the adduct [Ir(Bpq)$_2$(CzbpyCz)]PF$_6$·2F$^-$ and the absorption spectrum of [Ir(Bpq)$_2$(CzbpyCz)]PF$_6$ are shown in Figure S4 in the Supporting Information. There is a good spectral overlap between the PL emission spectrum of the free CzbpyCz ligand and the absorption spectrum of [Ir(Bpq)$_2$(CzbpyCz)]PF$_6$, which maybe ensures an efficient Förster energy transfer from the CzbpyCz ligand to the Ir complex. In addition, before binding with F$^-$ ions, the PL emission spectrum of the complex mainly showed a triplet emission from the Ir^{III} complex. Whereas the PL emission spectrum of the adduct [Ir(Bpq)$_2$(CzbpyCz)]PF$_6$·2F$^-$ showed a strong singlet emission from the CzbpyCz ligand and a weak emission at $\lambda = 572$ nm. Hence, we can think that the energy transfer becomes inefficient after binding with F$^-$ ions.

Hence, we can see that there is energy transfer from the CzbpyCz ligand to the Ir^{III} complex from the spectra properties, the emission-titration experiment, and theoretical calculation results. Before binding with F$^-$ ions, the energy transfer is efficient and only the triplet-state emission of the complex is observed (Scheme 2). However, binding with F$^-$ ions can inhibit the energy transfer, and the singlet emission from CzbpyCz is restored. Hence, the triplet–singlet dual emission can be switched through binding of F$^-$ ions.

Selectivity towards F$^-$ ions: High selectivity is necessary for an excellent chemosensor. Achieving high selectivity for the analyte of interest over a complex background of potentially competing species is, however, a challenge in sensor development. Herein, the selective coordination studies of the complex [Ir(Bpq)$_2$(CzbpyCz)]PF$_6$ were extended to other anions in CH$_3$CN. Only the addition of F$^-$ ions results in prominent changes of luminescence intensity at $\lambda = 584$ nm, whereas the addition of an excess of other anions (Cl$^-$, Br$^-$, I$^-$, ClO$_4$$^-$, NO$_3$$^-$, H$_2PO_4$$^-$, and CH$_3COO^-$) causes little or slight changes (Figure 11). Therefore, the complex displayed a high selectivity in sensing F$^-$ ions.

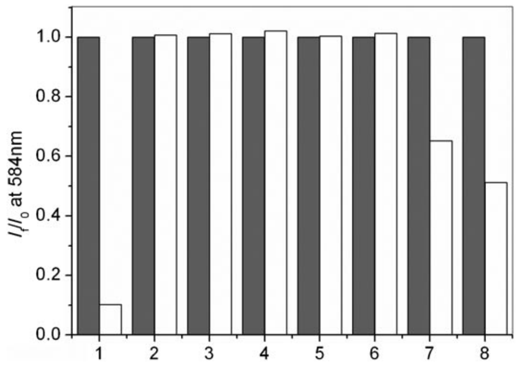

Figure 11. Emission response of [Ir(Bpq)$_2$(CzbpyCz)]PF$_6$ (20 μM) in the presence of various anions (4 equiv) in CH$_3$CN. Bars represent the emission intensity at $\lambda = 584$ nm. Gray and white represent I_{584} nm before and after the addition of anions, respectively. 1) F$^-$, 2) Cl$^-$, 3) Br$^-$, 4) I$^-$, 5) NO$_3$$^-$, 6) ClO$_4$$^-$, 7) H$_2PO_4$$^-$, 8) CH$_3COO^-$.

Conclusion

We have synthesized the novel cationic Ir^{III} complex $[Ir(Bpq)_2(CzbpyCz)]PF_6$, containing dimesitylboryl and carbazole groups, that has an intense absorption at $\lambda = 430$ nm with molar extinction coefficients of $\varepsilon > 10^4\,mol^{-1}\,dm^3\,cm^{-1}$ and displayed highly efficient orange/red phosphorescent emission at $\lambda = 584$ nm at room temperature. This Ir^{III} complex can be used as a highly selective phosphorescent probe for F^- ions. Binding of F^- ions to $[Ir(Bpq)_2(CzbpyCz)]PF_6$ quenched the phosphorescent emission from the Ir^{III} complex and switched on the fluorescent emission from the N^N ligand, which corresponds to a visual change in the emission color from orange-red to blue, thus enabling colorimetric as well as ratiometric fluoride ion sensing. Furthermore, phosphorescent detection of F^- ions excited with visible light was also realized. More importantly, the linear response of the change in the probe absorbance at $\lambda = 351$ nm versus the concentration of F^- ions allows efficient and accurate F^- quantification in the range 0–50 μM. We think that this result will be very useful for the further design of excellent phosphorescent ratiometric probes that utilize switchable triplet and singlet emissions.

Experimental Section

Characterization: NMR spectra were recorded on a Bruker Ultra Shield Plus 400 MHz NMR instrument (^{1}H: 400, ^{13}C: 100 MHz). The mass spectra were obtained on a Bruker autoflex MALDI-TOF/TOF mass spectrometer. The UV/Vis absorption spectra were recorded on a Shimadzu UV-3600 UV/Vis-NIR spectrophotometer. The PL spectra were measured using a RF-5301PC spectrofluorophotometer. The quantum efficiency for CzbpyCz was obtained under air using 9,10-diphenylanthracene as an external standard. The quantum efficiency for $[Ir(Bpq)_2(CzbpyCz)]PF_6$ was measured in degassed CH_2Cl_2 with fac-$[Ir(ppy)_3]$ (ppy = 2-phenylpyridine) as an external standard ($\Phi = 0.40$).

Theoretical calculations: The calculation was performed using the Gaussian 03 suite of programs.[15] The optimizations of the ligand and complex structures were performed by using B3LYP DFT. The LANL2DZ basis set was used to treat the iridium atom, whereas the 6–31G* basis set was used to treat all other atoms. The contours of the HOMOs and LUMOs were plotted.

Materials: All reagents, unless specified, were obtained from Sigma–Aldrich, Acros, and Alfa and were used as received. All solvents were purified before use. All the reactions were performed in a nitrogen atmosphere.

Synthesis

9-Hexylcarbazol-3-boronic acid: This compound was synthesized by using a reported procedure in a yield of 50 %.[16]

2-(4-Bromophenyl)quinoline (Brpq): This compound was synthesized by using a reported procedure in a yield of 75 %.[9]

2-[4-(Dimesitylboryl)phenyl]quinoline (Bpq): This compound was synthesized by using a reported procedure in a yield of 60 %.[10]

CzbpyCz: A degassed mixture of toluene ([monomer] = 0.25 M), aqueous potassium carbonate (2 M), and ethanol (2:1:1 v/v/v) was added to a mixture of 5,5′-dibromo-2,2′-bipyridine (0.16 g, 0.5 mmol), 9-hexylcarbazol-3-boronic acid (0.31 g, 1.05 mmol), and $[Pd(PPh_3)_4]$ (0.003 g, 0.0025 mmol). The reaction mixture was vigorously stirred at 70 °C for 12 h. The reaction mixture was cooled to room temperature, washed with brine, extracted with CH_2Cl_2 (3×), dried over anhydrous Na_2SO_4, and concentrated. The crude product was purified by column chromatography on silica gel with ethyl acetate/petroleum ether (1:3) as the eluent to yield a yellow solid. Recrystallization from CH_2Cl_2/hexane gave yellow crystals in 60 % yield. ^{1}H NMR (400 MHz, $CDCl_3$): $\delta = 9.08$ (d, $J = 2.03$ Hz, 2H; ArH), 8.56 (d, $J = 8.22$ Hz, 2H; ArH), 8.40 (d, $J = 1.43$ Hz, 2H; ArH), 8.15–8.20 (m, 4H; ArH) 7.81–7.78 (m, 2H; ArH), 7.55–7.44 (m, 6H; ArH), 7.31 (t, $J = 7.47$ Hz, 2H; ArH), 4.35 (t, $J = 7.20$ Hz, 4H; N$-CH_2$), 1.95–1.88 (m, 4H; CH_2), 1.46–1.26 (m, 12H; CH_2), 0.88 ppm (t, $J = 7.20$ Hz, 6H; CH_3); ^{13}C NMR (100 MHz, $CDCl_3$): $\delta = 154.20$, 147.98, 141.14, 140.58, 137.46, 135.35, 128.63, 126.30, 125.06, 123.80, 123.00, 121.10, 120.76, 119.38, 119.11, 109.53, 109.19, 43.48, 31.82, 29.21, 27.22, 22.79, 14.28 ppm.

$[Ir(Bpq)_2(CzbpyCz)]PF_6$: $[Ir(Bpq)_2(CzbpyCz)]PF_6$ was synthesized through a standard two-step procedure according a reported method.[6c] A mixture of 2-ethoxyethanol and water (3:1, v/v) was added to a flask containing $IrCl_3{\cdot}3H_2O$ (1 mmol) and Bpq (2.5 mmol). The reaction mixture was heated to reflux for 24 h. After cooling, an orange solid precipitate was removed by filtration to give the crude cyclometalated Ir^{III} chloro-bridged dimer. A solution of the cyclometalated Ir^{III} chloro-bridged dimer (0.079 mmol) and CzbpyCz (0.158 mmol) in CH_2Cl_2/MeOH (30 mL, 2:1 v/v) was heated to reflux. The red solution was cooled to room temperature after 4 h and a 10-fold excess of potassium hexafluorophosphate was added. The suspension was stirred for 2 h, filtered to remove any insoluble inorganic salts, and evaporated to dryness under reduced pressure. The crude product was purified with column chromatography on silica gel with CH_2Cl_2/acetone (50:1) as the eluent to afford an orange/yellow solid in 60 % yield. ^{1}H NMR (400 MHz, $CDCl_3$): $\delta = 8.58$–8.30 (m, 6H; ArH), 8.08–7.91 (m, 10H; ArH), 7.56–7.35 (m, 18H; ArH), 7.02 (s, 3H; ArH), 6.54–6.41 (m, 9H; ArH), 4.35 (t, $J =$ 6.85 Hz, 4H; N-CH_2), 2.24 (s, 12H; CH_3), 1.93–1.86 (m, 4H; CH_2), 1.67 (s, 24H; CH_3), 1.39–1.19 (m, 12H; CH_2), 0.88 ppm (t, $J = 6.91$ Hz, 6H; CH_3); ^{13}C NMR (100 MHz, $CDCl_3$): $\delta = 131.48$, 130.36, 128.99, 127.97, 127.85, 127.05, 126.81, 125.44, 125.12, 124.99, 124.81, 124.19, 124.00, 122.76, 120.77, 119.98, 118.47, 117.26, 110.02, 109.46, 43.56, 31.80, 29.19, 27.19, 23.16, 22.79, 21.51, 14.28 ppm; MS (MALDI-TOF) (m/z): 1753.0 $[M-PF_6]^+$.

Acknowledgements

This work was financially supported by the National Basic Research Program of China (973 Program, 2009CB930601), National Natural Science Foundation of China (project no. 50803028, 20804019, and 20774043), Natural Science Foundation of Jiangsu Province of China (BK2009427), Natural Science Fund for Colleges and Universities in Jiangsu Province (08 KJD430017), Scientific and Technological Innovation Teams of Colleges and Universities in Jiangsu Province (TJ207035 and TJ209035), Nanjing University of Posts and Telecommunications (project no. NY208045), and the Program for Postgraduates Research Innovations in University of Jiangsu Province (CX08B_084Z).

---

[1] a) K. L. Kirk, *Biochemistry of the Halogens and Inorganic Halides*, Plenum Press, New York **1991**, p. 58; b) B. L. Riggs, *Bone and Mineral Research,* Elsevier, Amsterdam, **1984**, p. 366; c) A. Wiseman, *Handbook of Experimental Pharmacology XX/2, Part 2*, Springer, Berlin **1970**, p. 48; d) P. Connet, *Fluoride* **2007**, *40*, 155–158; e) R. G. Foulkes, *Fluoride* **2007**, *40*, 229–237; f) S. Ayoob, A. K. Gupta, *Crit. Rev. Environ. Sci. Technol.* **2006**, *36*, 433–487; g) E. B. Bassin, D. Wypij, R. B. Davis, *Cancer Causes Control* **2006**, *17*, 421–428; h) Y. Yu, W. Yang, Z. Dong, C. Wan, J. Zhang, J. Liu, K. Xiao, Y. Huang, B. Lu, *Fluoride* **2008**, *41*, 134–138.

[2] a) Y. Kubo, M. Yamamoto, M. Ikeda, M. Takeuchi, S. Shinkai, S. Yamaguchi, K. Tamao, *Angew. Chem.* **2003**, *115*, 2082–2086; *Angew. Chem. Int. Ed.* **2003**, *42*, 2036–2040; b) Z. Q. Liu, M. Shi, F. Y. Li, Q. Fang, Z. H. Chen, T. Yi, C. H. Huang, *Org. Lett.* **2005**, *7*, 5481–5484; c) M. H. Lee, T. Agou, J. Kobayashi, T. Kawashima, F. P. Gabbaï, *Chem. Commun.* **2007**, 1133–1135; d) X. Y. Liu, D. R. Bai, S. Wang, *Angew. Chem.* **2006**, *118*, 5601–5604; *Angew. Chem. Int.*

Ed. **2006**, *45*, 5475–5478; e) K. Parab, K. Venkatasubbaiah, F. Jäkle, *J. Am. Chem. Soc.* **2006**, *128*, 12879–12885; f) S. Yamaguchi, S. Akiyama, K. Tamao, *J. Am. Chem. Soc.* **2001**, *123*, 11372–11375.

[3] a) P. D. Beer, P. A. Gale, *Angew. Chem.* **2001**, *113*, 502–532; *Angew. Chem. Int. Ed.* **2001**, *40*, 486–516; b) H. Miyaji, W. Sato, J. L. Sessler, *Angew. Chem.* **2000**, *112*, 1847–1850; *Angew. Chem. Int. Ed.* **2000**, *39*, 1777–1780; c) C. B. Black, B. Andrioletti, A. C. Try, C. Ruiperez, J. L. Sessler, *J. Am. Chem. Soc.* **1999**, *121*, 10438–10439; d) E. J. Cho, J. W. Moon, S. W. Ko, J. Y. Lee, S. K. Kim, J. Yoon, K. C. Nam, *J. Am. Chem. Soc.* **2003**, *125*, 12376–12377; e) M. Boiocchi, L. Del Boca, D. E. Gomez, L. Fabbrizzi, M. Licchelli, E. Monzani, *J. Am. Chem. Soc.* **2004**, *126*, 16507–16514; f) K. Chellappan, N. J. Singh, I. C. Hwang, J. W. Lee, K. S. Kim, *Angew. Chem.* **2005**, *117*, 2959–2963; *Angew. Chem. Int. Ed.* **2005**, *44*, 2899–2903.

[4] a) T. Agou, J. Kobayashi, T. Kawashima, *Inorg. Chem.* **2006**, *45*, 9137–9144; b) C. D. Entwistle, T. B. Marder, *Angew. Chem.* **2002**, *114*, 3051–3056; *Angew. Chem. Int. Ed.* **2002**, *41*, 2927–2931; c) M. Melaimi, F. P. Gabbaï, *J. Am. Chem. Soc.* **2005**, *127*, 9680–9681; d) T. W. Hudnall, F. P. Gabbaï, *J. Am. Chem. Soc.* **2007**, *129*, 11978–11986.

[5] a) P. Anzenbacher, Jr., D. S. Tyson, K. Jursikova, F. N. Castellano, *J. Am. Chem. Soc.* **2002**, *124*, 6232–6233; b) J. L. Fillaut, J. Andries, J. Perruchon, J. P. Desvergne, L. Toupet, L. Fadel, B. Zouchoune, J. Y. Saillard, *Inorg. Chem.* **2007**, *46*, 5922–5932; c) D. A. Jose, P. Kar, D. Koley, B. Ganguly, W. Thiel, H. N. Ghosh, A. Das, *Inorg. Chem.* **2007**, *46*, 5576–5584; d) L. Huynh, Z. Wang, J. Yang, V. Stoeva, A. Lough, I. Manners, M. A. Winnik, *Chem. Mater.* **2005**, *17*, 4765–4773; e) Q. Zhao, F. Y. Li, C. H. Huang, *Chem. Soc. Rev.* **2010**, DOI: 10.1039/B915340C.

[6] a) Q. Zhao, T. Y. Cao, F. Y. Li, X. H. Li, H. Jing, T. Yi, C. H. Huang, *Organometallics* **2007**, *26*, 2077–2081; b) Q. Zhao, S. J. Liu, F. Y. Li, T. Yi, C. H. Huang, *Dalton Trans.* **2008**, 3836–3840; c) Q. Zhao, F. Y. Li, S. J. Liu, M. X. Yu, Z. Q. Liu, T. Yi, C. H. Huang, *Inorg. Chem.* **2008**, *47*, 9256–9264; d) H. L. Chen, Q. Zhao, F. Y. Li, Y. B. Wu, H. Yang, T. Yi, C. H. Huang, *Inorg. Chem.* **2007**, *46*, 11075–11081.

[7] a) Y. You, S. Y. Park, *Adv. Mater.* **2008**, *20*, 3820–3826; b) S. B. Zhao, T. McCormick, S. Wang, *Inorg. Chem.* **2007**, *46*, 10965–10967; c) E. Sakuda, A. Funahashi, N. Kitamura, *Inorg. Chem.* **2006**, *45*, 10670–10677; d) Y. Sun, N. Ross, S. B. Zhao, K. Huszarik, W. L. Jia, R. Y. Wang, D. Macartney, S. Wang, *J. Am. Chem. Soc.* **2007**, *129*, 7510–7511; e) S. T. Lam, N. Y. Zhu, V. W. W. Yam, *Inorg. Chem.* **2009**, *48*, 9664–9670; f) Y. L. Rao, S. Wang, *Inorg. Chem.* **2009**, *48*, 7698–7713; g) Z. M. Hudson, S. B. Zhao, R. Y. Wang, S. Wang, *Chem. Eur. J.* **2009**, *15*, 6131; h) Y. Sun, S. Wang, *Inorg. Chem.* **2009**, *48*, 3755.

[8] N. Miyaura, A. Suzuki, *J. Chem. Soc. Chem. Commun.* **1979**, 866–867.

[9] Y. Z. Hu, G. Zhang, R. P. Thummel, *Org. Lett.* **2003**, *5*, 2251–2253.

[10] R. Stahl, C. Lambert, C. Kaiser, R. Wortmann, R. Jakober, *Chem. Eur. J.* **2006**, *12*, 2358–2370.

[11] K. Nonoyama, *Bull. Chem. Soc. Jpn.* **1974**, *47*, 467–468.

[12] a) K. A. King, P. J. Spellane, R. J. Watts, *J. Am. Chem. Soc.* **1985**, *107*, 1431–1432; b) S. Lamansky, P. Djurovich, D. Murphy, F. Abdel-Razzaq, R. Kwong, I. Tsyba, M. Bortz, B. Mui, R. Bau, M. E. Thompson, *Inorg. Chem.* **2001**, *40*, 1704–1711.

[13] a) A. Tsuboyama, H. Iwawaki, M. Furugori, T. Mukaide, J. Kamatani, S. Igawa, T. Moriyama, S. Miura, T. Takiguchi, S. Okada, M. Hoshino, K. Ueno, *J. Am. Chem. Soc.* **2003**, *125*, 12971–12979; b) A. B. Tamayo, S. Garon, T. Sajoto, P. I. Djurovich, I. M. Tsyba, R. Bau, M. E. Thompson, *Inorg. Chem.* **2005**, *44*, 8723–8732.

[14] Q. Zhao, S. J. Liu, M. Shi, C. M. Wang, M. X. Yu, L. Li, F. Y. Li, T. Yi, C. H. Huang, *Inorg. Chem.* **2006**, *45*, 6152–6160.

[15] Gaussian 03, Revision C.02, M. J. Frisch, G. W. Trucks, H. B. Schlegel, G. E. Scuseria, M. A. Robb, J. R. Cheeseman, J. A. Montgomery, Jr., T. Vreven, K. N. Kudin, J. C. Burant, J. M. Millam, S. S. Iyengar, J. Tomasi, V. Barone, B. Mennucci, M. Cossi, G. Scalmani, N. Rega, G. A. Petersson, H. Nakatsuji, M. Hada, M. Ehara, K. Toyota, R. Fukuda, J. Hasegawa, M. Ishida, T. Nakajima, Y. Honda, O. Kitao, H. Nakai, M. Klene, X. Li, J. E. Knox, H. P. Hratchian, J. B. Cross, V. Bakken, C. Adamo, J. Jaramillo, R. Gomperts, R. E. Stratmann, O. Yazyev, A. J. Austin, R. Cammi, C. Pomelli, J. W. Ochterski, P. Y. Ayala, K. Morokuma, G. A. Voth, P. Salvador, J. J. Dannenberg, V. G. Zakrzewski, S. Dapprich, A. D. Daniels, M. C. Strain, O. Farkas, D. K. Malick, A. D. Rabuck, K. Raghavachari, J. B. Foresman, J. V. Ortiz, Q. Cui, A. G. Baboul, S. Clifford, J. Cioslowski, B. B. Stefanov, G. Liu, A. Liashenko, P. Piskorz, I. Komaromi, R. L. Martin, D. J. Fox, T. Keith, M. A. Al-Laham, C. Y. Peng, A. Nanayakkara, M. Challacombe, P. M. W. Gill, B. Johnson, W. Chen, M. W. Wong, C. Gonzalez, J. A. Pople, Gaussian, Inc., Wallingford, CT, **2004**.

[16] a) H. Y. Wang, G. Chen, Y. Liu, L. H. Hu, X. P. Xu, S. J. Ji, *Dyes Pigm.* **2009**, *83*, 269–275; b) W. L. Yu, J. Pei, Y. Cao, W. Huang, A. J. Heeger, *Chem. Commun.* **1999**, 1837–1838.

Received: February 10, 2010